DERIVATION OF MARS ATMOSPHERIC DUST OPACITIES FROM RADIATIVE TRANSFER ANALYSIS OF VIKING IRTM EMISSION PHASE FUNCTION SEQUENCES;

R.T. Clancy and S.W. Lee, Laboratory for Atmospheric and Space Physics, University of Colorado, Boulder, CO 80309

During the span of the Viking Orbiter missions, several hundred emission-phase-function (EPF) sequences were obtained, in which the IRTM instrument observed the same area of surface as the spacecraft moved overhead. The IRTM data set as a whole is well calibrated, having been corrected for inter-spacecraft, inter-detector, and temporal calibration variations; a conservative estimate for the absolute uncertainty inherent in this data set is 1-2% [1]. The EPF visual brightness observations (passband of 0.3-3.0 μm) present very accurately calibrated albedos of a given region and the atmosphere above it versus emission (and to a lesser extent, incidence) angle. Although these observations were designed for the purposes of surface photometric analyses, they are quite suitable for the derivation of atmospheric dust opacities. The IRTM EPF sequences are most sensitive to the atmospheric dust loading over regions of low surface albedo where the effects of dust scattering for even low dust opacities ($\tau \leq .2$) are distinctive at high emission angles.

We have developed a radiative transfer model of the Mars atmosphere and surface based upon a discrete-ordinates radiative transfer code [2]. Input parameters include the atmospheric dust opacity, the single scattering albedo and particle phase function of atmospheric dust, and the surface bidirectional reflectance. We incorporate the latest Mars dust scattering parameters from Pollack and co-workers (Pollack, personal communication, 1989) for aspherical particles, which are characterized by a scattering asymmetry parameter of .56 and a single scattering albedo of .86. A 16-stream approximation is adopted to provide adequate representation of the Pollack dust phase function. The surface photometric function is estimated from EPF sequences at low dust opacities and emission angles, where the effects of scattering by atmospheric dust are minimized. The exact behavior of the bidirectional reflectance at large emission angles is not critical since the contribution of atmospheric dust scattering dominates the observed reflectance in this region.

In Figures 1 and 2, below, we show fits of normalized reflectance versus emission curves to the EPF observations of a bright and dark region within Cerberus. The various model lines indicate a range of atmospheric dust opacities; the long-dashed line ($\tau = 0$) indicates the bidirectional reflectance adopted for the surface at the near-zero incidence angle of these observations. Notice that the net-effect of atmospheric dust is to increase the observed reflectance of the dark region, and decrease the observed reflectance of the bright region. Furthermore, there are distinctly different emission-angle dependences for the bright and dark regions. For both regions, the best agreement between model and data corresponds to an atmospheric dust opacity of ~0.2. The similar values for dust opacity are consistent with the similar locations of these regions (within 1-2 degrees of longitude and latitude of one another), and the contemporaneous observation of the two regions. Furthermore, a value of 0.2 is roughly consistent with the value of .07 for the IRTM infrared opacity given by Martin [3] for this local and L_S. The exact scaling between infrared and visible (the EPF data are at an effective wavelength of 0.57 μm) dust opacities depends on the dust particle and compositional parameters. Martin [3] finds a ratio of 2-2.5 between his infrared opacities and the Viking Lander visible opacities [4].

We present a much broader range of EPF derived dust opacities versus locale and L_S, including point-by-point comparisons with the Martin [3] infrared opacities. We also present a subset of high phase angle/ high dust opacity observations which provide additional constraints on the dust scattering characteristics.

REFERENCES: [1] Pleskot, L.K., and E.D. Miner (1981). Time variability of martian bolometric albedo. *Icarus 45*, 179-201. [2] Stamnes, K., S.C. Tsay, W. Wiscombe, and K. Jayaweera (1988). A numerically stable algorithm for discrete-ordinate-method radiative transfer in scattering and emitting layered media. *Appl. Opt., 27*, 2502-2509. [3] Martin, T. Z. (1986). Thermal infrared opacity of the Mars atmosphere. *Icarus, 66*, 2-21. [4] Pollack, J. B., D. S. Colburn,.F. M. Flasar, R. Kahn, C. E. Carston, and D. Pidek (1979). Properties and effects of dust particles suspended in the martian atmosphere. *J. Geophys. Res., 84*, 2929-2945.

MARS ATMOSPHERIC DUST OPACITIES: R.T. Clancy and S.W. Lee

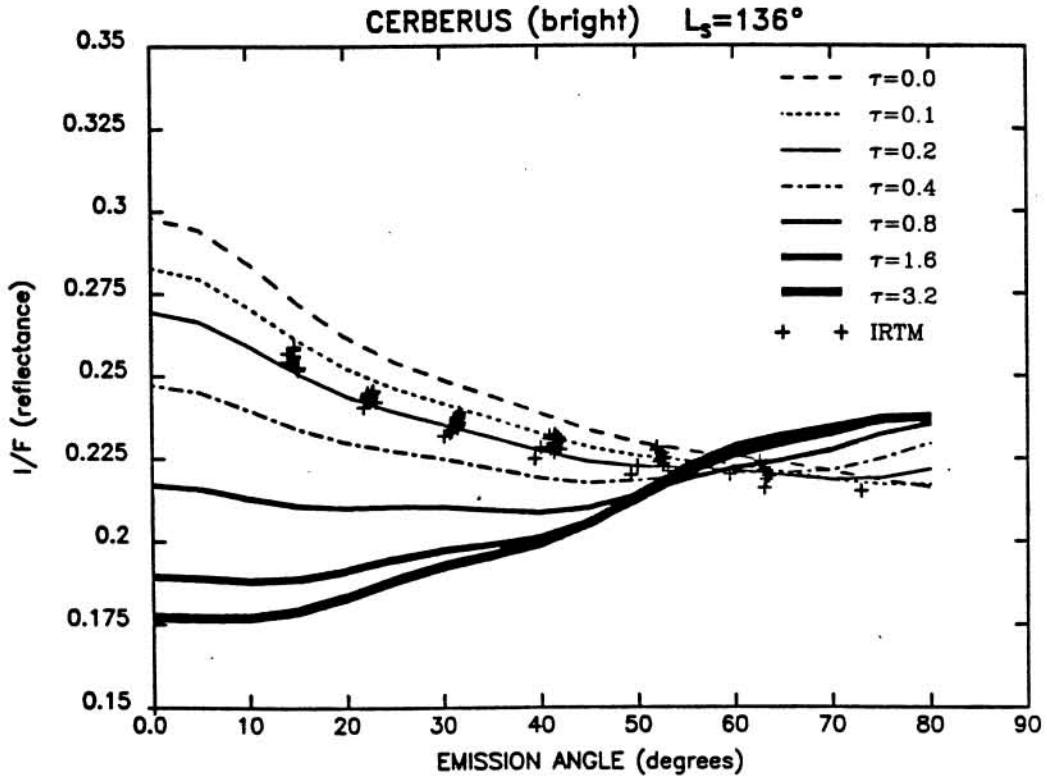

Figure 1: Reflectance vs emission angle for an sequence over a bright region in Cerberus (crosses). Radiative transfer calculations versus atmospheric dust opacity are presented by the various lines.

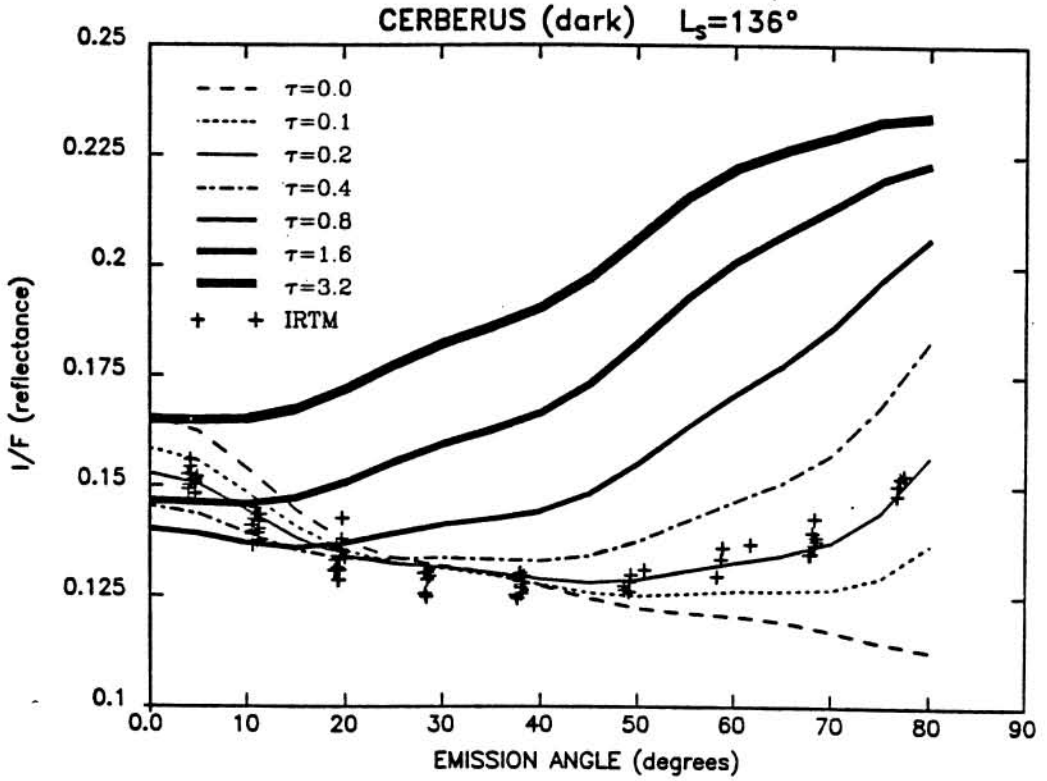

Figure 2: Reflectance vs emission angle for an EPF sequence over a dark region in Cerberus (crosses). Radiative transfer calculations versus atmospheric dust opacity are presented by the various lines.